

See discussions, stats, and author profiles for this publication at:
<https://www.researchgate.net/publication/257546357>

Preparation of superhydrophobic electroconductive graphene-coated cotton cellulose

ARTICLE *in* CELLULOSE · APRIL 2013

Impact Factor: 3.57 · DOI: 10.1007/s10570-013-9873-y

CITATIONS

23

READS

330

2 AUTHORS:



[Mohammad Shateri-Khalilabad](#)

Islamic Azad University, Yazd Branch, Y...

18 PUBLICATIONS 300 CITATIONS

SEE PROFILE



[Mohammad Esmail Yazdanshenas](#)

Islamic Azad University

90 PUBLICATIONS 735 CITATIONS

SEE PROFILE

Preparation of superhydrophobic electroconductive graphene-coated cotton cellulose

Mohammad Shateri-Khalilabad ·
Mohammad E. Yazdanshenas

Received: 4 November 2012 / Accepted: 24 January 2013 / Published online: 5 February 2013
© Springer Science+Business Media Dordrecht 2013

Abstract A simple and versatile method based on cotton cellulose coated with graphene is reported for the fabrication of superhydrophobic and electroconductive textiles. Graphene oxide was deposited on cotton fibers by a dip-pad-dry method followed by reduction with ascorbic acid to yield a fabric with a layer of graphene. The fabric was then reacted with methyltrichlorosilane to form polymethylsiloxane (PMS) nanofilaments on the fibers surface. The surface chemistry and morphology were characterized by UV–visible reflectance spectrophotometry, Fourier transform infrared spectroscopy, energy-dispersive X-ray spectroscopy and scanning electron microscopy. The water contact angle (CA)/shedding angle (SHA) and resistivity measurements were used for assessing hydrophobicity and conductivity, respectively. The graphene-coated fabric showed hydrophobicity with the CA of $143.2^\circ \pm 2.9^\circ$ and SHA of 41° . The formation of PMS nanofilaments displayed superhydrophobicity with CA of $163^\circ \pm 3.4^\circ$ and SHA of 7° , which indicated the self-cleaning ability. Conductivity of the graphene-coated fabric was confirmed by the electrical resistivity of $91.8 \text{ k}\Omega/\text{sq}$ which

increased to $112.5 \text{ k}\Omega/\text{sq}$ after the formation of PMS nanofilaments.

Keywords Cotton · Cellulose · Superhydrophobic · Electroconductive · Graphene · Self-cleaning

Introduction

Superhydrophobic surfaces have attracted tremendous attention over the last decade in both academic and commercial contexts due to their wide applicability in different fields. Along with the development of fabrication techniques, the promising application of superhydrophobic surfaces has been extended from the primary objectives in self-cleaning, anti-sticking, anti-fouling and low-friction coatings to the new advanced areas such as oil–water separation, high-performance optics, microfluidic channels, Janus interface materials, tunable wettable surface, super water proof textiles and multifunctional materials (Yan et al. 2011; Ganesh et al. 2011; Pereira et al. 2011; Cervin et al. 2012; Simončič et al. 2012; Athauda and Ozer 2012; Shateri Khalil-Abad and Yazdanshenas 2010; Peng et al. 2012).

Recent advances in material science and nanotechnology with the combination of unique properties of fibers has caused the emergence of advanced textiles (Saini et al. 2012; Hu and Cui 2012; Zou et al. 2012; Hu et al. 2010, 2012a, b; Yu et al. 2011). The creation of electrical conductivity feature to the textile

Electronic supplementary material The online version of this article (doi:10.1007/s10570-013-9873-y) contains supplementary material, which is available to authorized users.

M. Shateri-Khalilabad (✉) · M. E. Yazdanshenas
Department of Textile Engineering, Yazd Branch,
Islamic Azad University, Yazd, Iran
e-mail: m.shaterikha@iauyazd.ac.ir;
shaterimagenta@gmail.com

substrates is an essential key for the fabrication of such advanced fibrous materials. Conductivity has been provided by various materials such as conjugated polymers, carbon nanotubes and indium tin oxide. But, the most widely used methods require complex processes, expensive materials and pre-functionalization and have some disadvantages such as lacking uniform coating, flexibility, and durable wear-resistance, which increase the cost of production.

Graphene has recently gained intense interest owing to its outstanding mechanical, thermal, optical, electronic, and excitonic properties (Huang et al. 2011; Allen et al. 2009). Graphene with high electrical conductivity can serve as new nanoscale building blocks to create unique electroconductive materials. Graphene has been used on paper-like materials (Luong et al. 2011; Chen et al. 2008) or dispersed throughout a polymeric matrix (Huang et al. 2012; Tang et al. 2011, 2012) to make electrically conductive composites. Therefore, it can be also used on cellulosic textile materials as an electroconductive coating. On the other hand, hydrophilicity characteristic of cellulose makes it sensitive to water or moisture adsorption, which causes interference with electroconductivity. Thus, hydrophobicity modification could be a solution for this problem.

In this paper, graphene was used as a conductive material and polymethylsiloxane (PMS) nanostructures as a rough low-surface energy layer for the fabrication of superhydrophobic electroconductive cotton fabric. Graphene oxide (GO) was immobilized on the surface of cotton fabric through a conventional dip-pad-cure approach. The GO was then chemically reduced to the conductive graphene. At the end, the PMS coating was formed by reacting the graphene-coated cotton with the methyltrichlorosilane (MTCS). To the best of our knowledge, this is the first report on the fabrication of superhydrophobic surface on electroconductive graphene-coated cotton.

Materials and methods

Materials

Graphite purum powder (particle size <100 μm) was purchased from Fluka. All other materials including potassium permanganate (KMnO_4), ascorbic acid ($\text{C}_6\text{H}_8\text{O}_6$), sodium hydroxide (NaOH), MTCS, sulfuric acid (H_2SO_4 , 98 %), hydrochloric acid (HCl , 37 %),

hydrogen peroxide (H_2O_2 , 30 %), and n-hexane (99 %) were supplied by Merck. Desized, scoured and bleached 100 % cotton fabric was used as the substrate. Milli-Q grade (resistivity of $18.2 \text{ M } \Omega \text{ cm}^{-1}$) water was used throughout the experiments.

Preparing GO

GO was synthesized using a modified Hummer's method (Hummers and Offeman 1958). One g of as-purchased graphite powder was added to 25 ml of H_2SO_4 and left stirring for 12 h at ambient temperature. While keeping the temperature less than 10°C , 3.5 g of KMnO_4 was added and stirred at 50°C for 2 h. Then, 70 ml distilled water and 5 ml H_2O_2 were added and the mixture was stirred for 30 min. For purification, the resulting mixture was centrifuged, rinsed first with 5 % HCl solution and then with deionized water (three times). 200 ml of water was added to the resulting product to make 0.5 % w/v dispersion. The dispersion was exfoliated acoustically using a Euronda bath sonicator (Eurosonic 4D, 50–60 Hz) with a power of 350 W for 60 min. This 0.5 % aqueous dispersion was used to prepare all the subsequent dispersions for deposition.

Preparing the GO-coated cotton

Aqueous dispersion of GO with the concentration of 0.2 mg ml^{-1} was prepared from stock dispersion. Cotton fabric was immersed into the GO dispersion for 10 min, then removed and subsequently padded with the wet pick up of 100 %. This process was repeated three times to increase the GO loading on the cotton fibers. The fabric was subsequently dried at $70\text{--}80^\circ\text{C}$ for 60 min. The obtained fabric was coded as GO-cotton.

Preparing the graphene-coated cotton

The GO-cotton samples (1 g) were immersed into 100 ml solution of 0.05 M $\text{C}_6\text{H}_8\text{O}_6$. The mixture was kept at 95°C for 60 min with constant stirring. The resulting fabrics were removed and rinsed with copious amount of water to remove the remaining reducing agent. At the end, the fabrics were dried in an oven at $70\text{--}80^\circ\text{C}$ for 60 min. The obtained fabrics were coded as graphene-cotton. The amount of the graphene deposited on the fabric was determined by reweighing fabric after drying for 1.5 h in an oven at

80 °C. An analytical balance (Scatec SBA32) with 10^{-4} precision was used to measure the samples' weight.

Surface modification by MTCS

The graphene-cotton sample was modified by immersing the fabric into the MTCS solution of n-hexane and reacted for 15 min under constant stirring. After the reaction, the sample was removed, washed with acetone-ammonia and then with tap water. The obtained sample was dried and cured in an oven at 110 °C for 60 min. The sample was coded as PMS-graphene-cotton.

Characterization

Transmission electron microscopy characterization of graphene oxide was performed using a microscope LEO 912AB with the accelerating voltage of 120 kV. A droplet of GO dispersion was cast onto a TEM copper grid and the solvent was evaporated overnight at room temperature. The reflectance spectra of the fabrics were measured using a Perkin-Elmer Lambda 35 UV–visible spectrophotometer. Fourier Transform Infrared (FTIR) spectra were recorded on a Bruker Equinox 55 FTIR spectrometer in ATR mode. Surface morphology of the fabrics was examined by a KYKY-EM3200 scanning electron microscope, after sputter coating with a very thin layer of Au. The static water contact angle (CA) measurements were completed on a self-developed goniometer apparatus coupled to a high resolution camera (Shirgholami et al. 2011). Water droplets of 5 μ l were used in the CA tests. For statistics, 6 separate measurements were performed at different locations on the fabric surface and the results

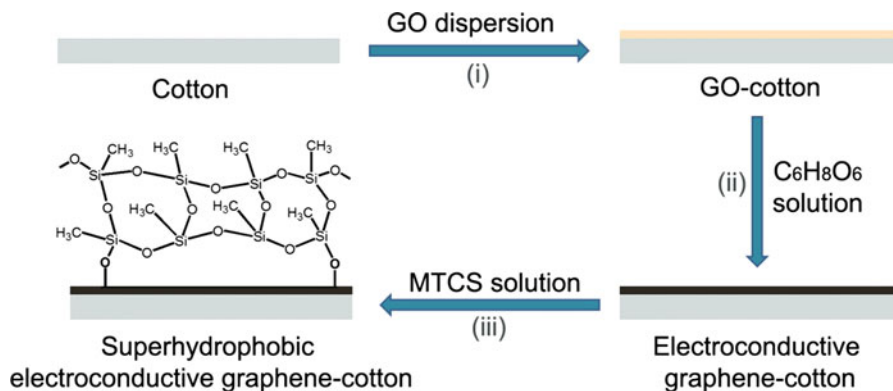
were averaged to obtain the mean and standard deviation. Water shedding angle (SHA) was determined based on the method of Zimmermann et al. (2009). The water SHA was determined for 10 μ l water droplets and 2 mm needle–substrate distance. Electrical surface resistivity of the fabrics was measured using a standard two-probe method (AATCC Technical Manual 2007) by means of Sa-Iran digital multimeter model 8515.

Results and discussion

The present approach for making superhydrophobic electroconductive graphene-coated cotton fabric involved three key steps, as shown in Fig. 1. The first was to coat cotton fibers with GO which were obtained from graphite powders by Hummer's method (Hummers and Offeman 1958). The coating was applied by a simple dip-pad-dry process, which is widely used in the textile industry for finishing fabrics (Schindler and Hauser 2004). The second was to reduce the GO-cotton with ascorbic acid to convert GO into the conductive graphene. Finally, low surface energy PMS layer was formed on the graphene-coated sample.

GO is a material prepared by acid-treating graphite which consists of graphene decorated with epoxides, hydroxyl, carbonyl and carboxyl groups on its basal planes and edges (Park et al. 2008; Li et al. 2011). GO is highly exfoliated, dispersible and very stable when dispersed in water. Figure 2 shows TEM images of a typical GO nanosheet deposited on a standard TEM grid. The sheet was several micrometers in dimension with the wrinkled (rough) surface texture. High-resolution TEM image clearly illustrated the amorphous nature of the GO nanosheet.

Fig. 1 Three key steps for preparing superhydrophobic electroconductive cotton cellulose. (i) conformal coating of GO (brownish color) onto cotton fibers; (ii) conversion of GO layer into the electroconductive graphene layer (black color) via chemical reduction; (iii) coating of PMS nanostructures on the graphene-coated cotton. (Color figure online)



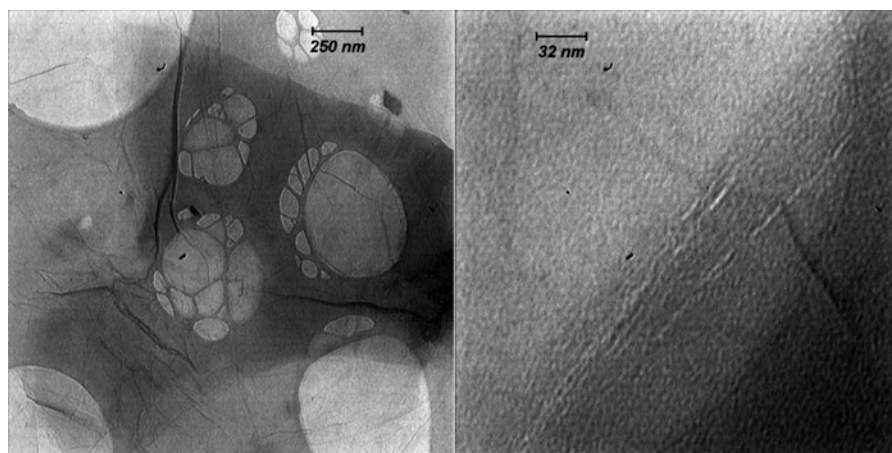


Fig. 2 TEM image of a typical GO sheet. The image on the right is in high-resolution

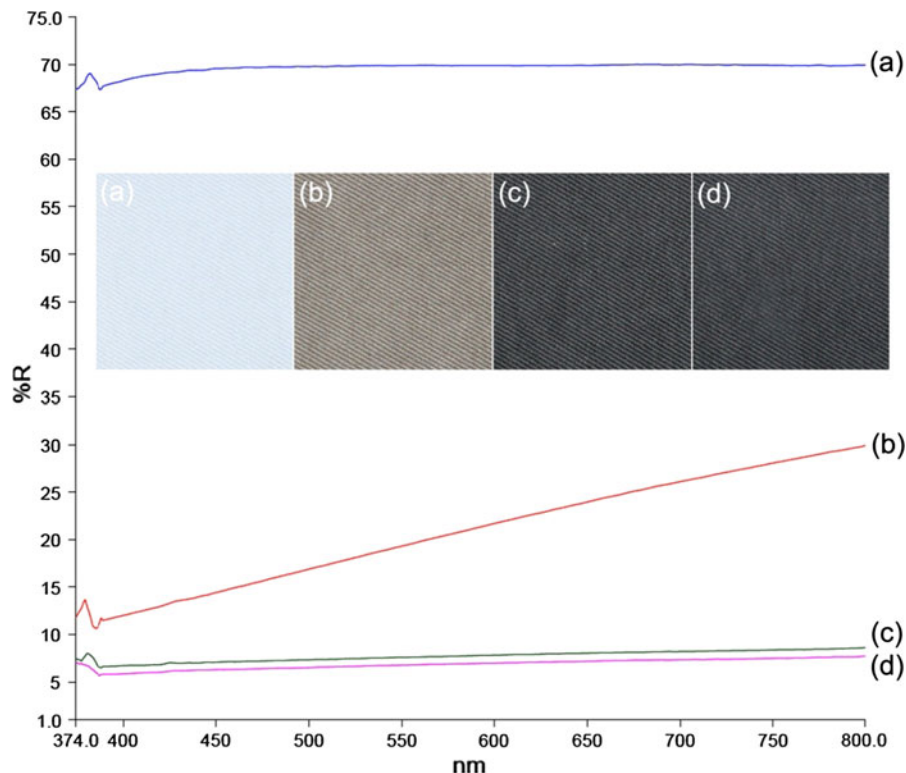
When the cotton fabric was dipped into the GO dispersion, it was quickly coated with the GO sheets because of van der Waals forces and hydrogen bonds between exfoliated GO and cellulose fibers. Consequently, the GO could be strongly adhered to the surface of the cotton cellulose during immersion. The GO content of the fabric was determined to be 5 g/kg.

In particular, color can be potentially employed as a fast and intuitive way for easy detection and simple evaluation of the deposition/reduction of GO on the surface of fabrics. The reflectance spectra of the fabrics in the ranges of 375–800 nm and their correspondence digital photographs are shown in Fig. 3. Digital photographs clearly showed color changes of the original fabric coated with the GO/graphene. As expected, deposition of the GO on the cotton fabric was accompanied by its color change from white to pale brown due to brownish color of the GO aqueous dispersion. After chemical reduction, the color change to graphitic black confirmed that GO was successfully transformed into graphene. This color change has been suggested as partial restoration of the π network within the carbon structure and has been witnessed through chemical reduction of the GO (Li et al. 2011). Uniform color of the graphene-cotton fabric showed that graphene sheets were homogeneously coated on the fabric surface. UV–visible spectra of the fabrics are consistent with the digital photographs that further demonstrated the successful deposition of the GO/graphene on the fabric. After surface modification with the MTCS, no significant changes were observed in the photograph of the

graphene-cotton. However, there was little difference between the spectra of the graphene-cotton and the PMS-graphene-cotton samples so that the reflectance percentage of the PMS-graphene-cotton sample was a little less due to the formation of PMS layer. The results of visual observation and spectrophotometry study established the affluent deposition of the GO, its reduction to the graphene and also the formation of PMS layer on the surface of fabric.

FTIR spectroscopy was used to identify the presence of functional groups on the solid surface of the treated fabrics. Fig. S1 shows FTIR spectra of the original cotton, the GO-cotton, the graphene-cotton and the PMS-graphene-cotton samples. FTIR spectra of all the samples showed characteristic bands for cellulose: the hydrogen bonded OH stretching at ca. 3,500–3,000 cm^{-1} , the CH stretching at 2,900 cm^{-1} , the OH bending at 1,635 cm^{-1} , the CH_2 bending at 1,430 cm^{-1} , the CH bending at 1,380 cm^{-1} , the C–O stretching at 1,058 cm^{-1} and 1,035 cm^{-1} , the CH bending or CH_2 stretching at 900 cm^{-1} . FTIR spectra of the GO-cotton and the graphene-cotton samples were quite similar to those of the original sample. No new peaks appeared in the treated samples, indicating that no chemical reactions occurred between the GO/graphene and cotton cellulose. Compared to these spectra, the spectrum of the PMS-graphene-cotton sample showed two new absorption peaks located at 781 and 1,273 cm^{-1} , which could be attributed to the stretching vibrations of the Si–C bands and to $-\text{CH}_3$ deformation vibrations of the siloxane compounds, respectively. The typical absorption peaks of the Si–O–Si bands of the siloxane

Fig. 3 The reflectance spectra of (a) the original cotton; (b) the GO-cotton; (c) the graphene-cotton; (d) the PMS-graphene-cotton. The images on the middle are the correspondence digital photographs of the fabrics showing their color changes



compounds in the $1,000\text{--}1,130\text{ cm}^{-1}$ region appeared to be overlapped by the cellulose bands due to C–O bending modes. These results indicated the successful reaction of the graphene-cotton fabric with the MTCS.

The chemical composition of the fabrics surface was characterized using EDS analysis. The EDS spectra are shown in Fig. S2–S4 and the detailed element content of the fabrics is summarized in Table S1. As shown in Fig. S2–S4, C and O are major elements in the original, the GO-cotton and the graphene-cotton fabrics. The data in Table S1 demonstrates the percent of C and O that did not change significantly due to the presence of the same elements in the GO. However, for the graphene-cotton fabric, the O content decreased markedly, which indicated that the oxygen functionalities of the GO were removed after reduction. The EDS spectrum of the PMS-graphene-cotton revealed a new Si peak originating from the MTCS. All the above results clearly indicated that the GO was converted into the graphene and the MTCS was successfully incorporated on the surface of the graphene-cotton fibers.

Electron microscopy was used to observe the morphology changes of the fabrics. Figure 4a–c are

the SEM images of the original, graphene-cotton and PMS-graphene-cotton samples, respectively. Significant change in surface morphology of the graphene-cotton fibers (Fig. 4b) was not recognized compared to the original sample (Fig. 4a), which was due to the very low thickness of the synthesized GO nanosheets (see Fig. 2, TEM images) and the low graphene content (3.4 g/kg) of the fabric, in which the graphene layer was not very visible from the SEM images. However, high-magnification image demonstrated smoother surface of the graphene-cotton due to the conformal coating of graphene. The conformal coating was largely due to very low thickness and size uniformity of graphene together with the strong adhesion between the graphene and cotton cellulose fibers. Also, a few numbers of white spots could be observed in some parts of the fibers (Fig. 4b, two representative white spots indicated by the black arrows) due to incomplete exfoliation of graphite particles during the synthesis process.

The SEM image of the PMS-graphene-cotton sample revealed the formation of PMS nanofilaments (Fig. 4c) that grew along the whole length of every cellulose fiber which made its surface rougher. The

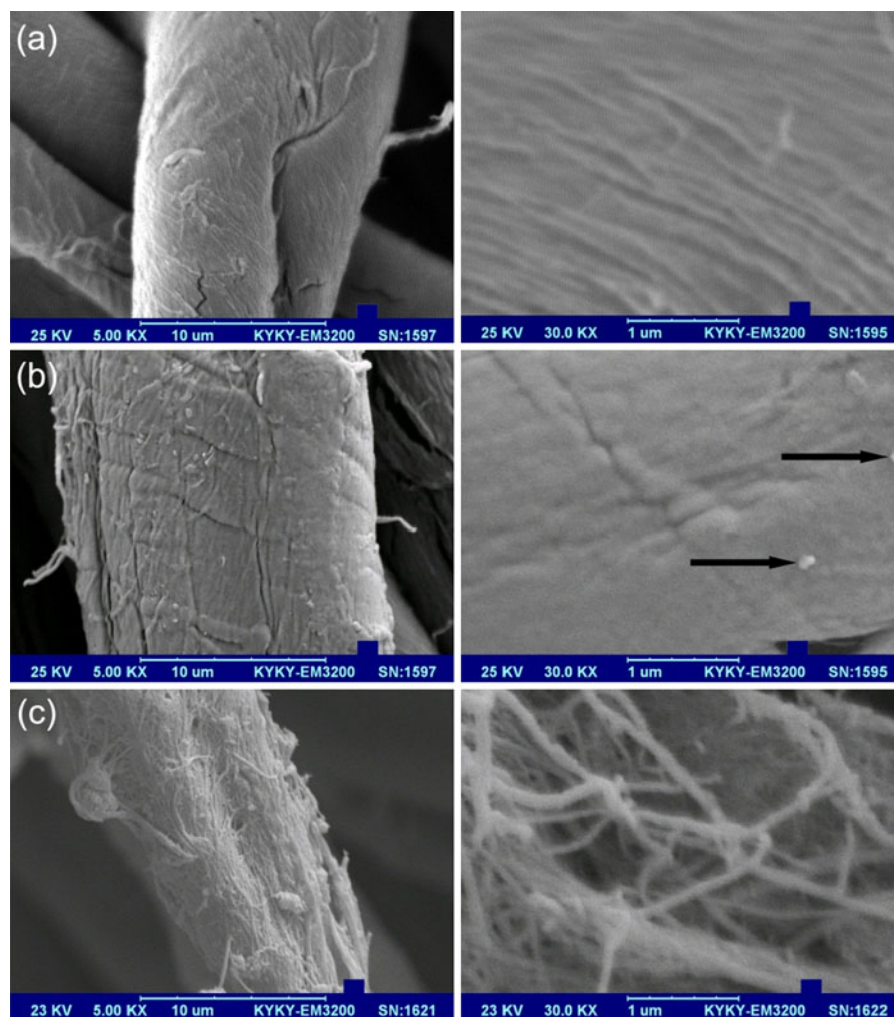


Fig. 4 SEM images of **a** the original cotton; **b** the graphene-cotton; **c** the PMS-graphene-cotton. The right images are at higher magnification

PMS content of the fabric was determined to be 18.6 g/kg. From the high-magnification image, it can be clearly seen that the coating consisting of the entangle PMS nanofilaments had feature length of several micrometer and diameter range of 30–90 nm. The formation of this special feature was the result of MTCS reaction with hydroxyl groups of cotton fabric and its polymerization and polycondensation under the applied condition (Shirgholami et al. 2013).

The wetting properties of the fabrics were analyzed by measuring water droplet CA and SHA. Cotton fabrics were composed of cellulose fibers having abundant surface hydroxyl groups. Therefore, they quickly absorbed water droplets (Fig. 5a). After coating of fabric with GO, the fabric showed a similar

wetting behavior when contacted with water droplets, indicating that the GO deposition did not change the well-known superhydrophilic property of cotton fabric. This was due to the presence of sufficient oxygenated functional groups (e.g., epoxides, hydroxyls, carboxylic acids) on the basal planes and edges of the GO (Park et al. 2008; Li et al. 2011). But, the graphene-cotton sample had a hydrophobic surface. Figure 5b shows the photograph of red colored water droplets placed on the graphene-cotton sample and the corresponding static water CA. The droplets formed a semi-circular shape after placing on the fabric surface. Water droplets placed on the sample were quite stable and the droplets could maintain their shapes for a long period of time showing complete covering of the

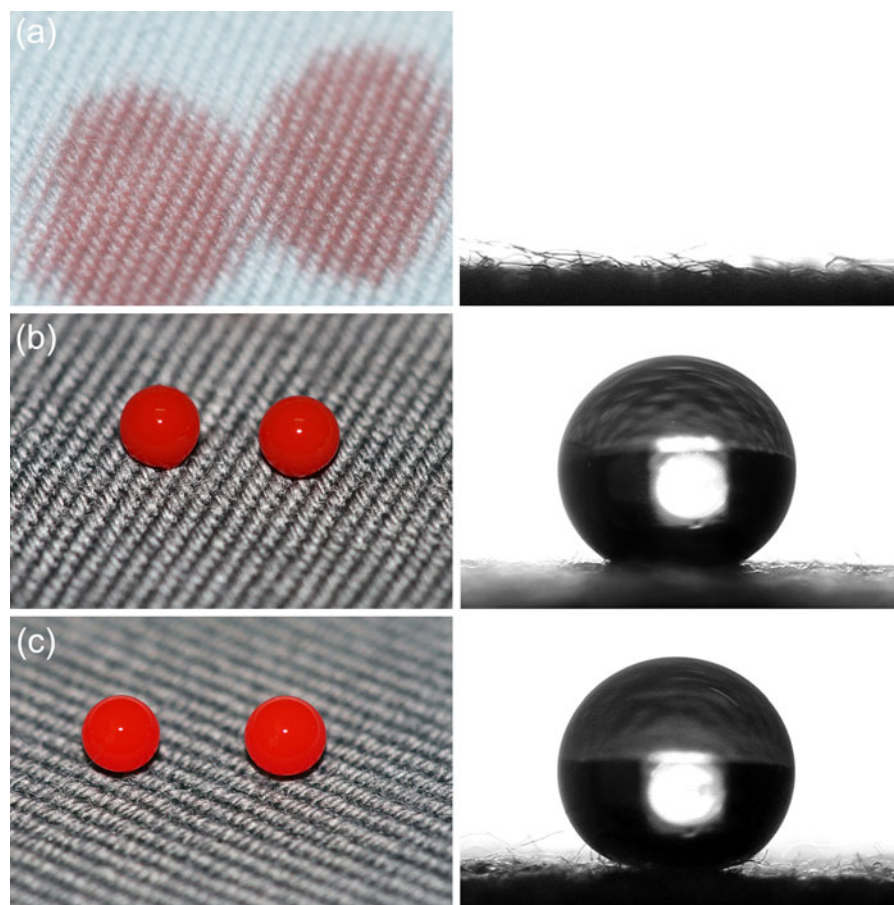


Fig. 5 Red-dyed water droplets sitting on **a** the original cotton; **b** the graphene-cotton; **c** the PMS-graphene-cotton. The images on the right show corresponding goniometer images for 5 µl droplets

fabric surface with the graphene. The results of CA and SHA measurements are listed in Table 1. For the graphene-cotton sample, the average CA of $143.2^\circ \pm 2.9^\circ$ was obtained, which indicated that the superhydrophilic cotton fabric turned into hydrophobic substrate as a result of the coating of cellulose fibers with the graphene. Hydrophobic characteristic of the graphene-cotton fabric was due to the removal of oxygen-containing groups during chemical reduction, which rendered the graphene hydrophobic (Lin et al. 2011; Wang et al. 2012). The same result was observed on the surface of the monolayer or few-layer graphene film with the thickness of 0.8–1.6 nm (Wang et al. 2009). However, compared to the CA value of the $127.0^\circ \pm 4.0^\circ$ for the graphene film, the observed value of CA for the graphene-cotton fabric was much higher because the cotton fabric consisted of a number of intersections of microscale cellulose fibers with the

mean diameter of 10–15 µm (see SEM images) which worked as the primary roughness for improving the water-repellency by the trapping of air pockets between the droplets and the cellulose fibers. For this sample, the water droplets adhered firmly to the surface and could resist against their gravitational forces at any tilting angles, indicating that a strong adhesive effect existed between the water droplets and the sticking surface of the graphene-coated fabrics. The high level of adhesion of water droplets to the fabric surface was also determined by the water SHA of 41° . This high adhesive force came from the smooth surface of the graphene-cotton fibers (see Fig. 4b) in which droplets could have a high contact area with the fibers surface. This hypothesis was demonstrated by removing the droplets from the fabric (the data were not shown) and observing the contact area of the droplet/fabric. It was observed that droplets wetted the

Table 1 Water CA and water SHA of the original, the graphene-cotton and the PMS-graphene-cotton

Sample	Water CA	Water SHA
Original cotton	0.0	—
Graphene-cotton	143.2° ± 2.9°	41°
PMS-graphene-cotton	163.0° ± 3.4°	7°

fabric surface but were not adsorbed into it. These results showed that the graphene-cotton fabric had a hydrophobic surface without self-cleaning properties.

Generally, two strategies have been used to create a superhydrophobic surface: (a) introduction of micro/nanoscale hierarchical roughness or porosity on a low surface energy material and (b) creation of micro/nanoscale hierarchical roughness on surface, followed by deposition of a low surface energy material on top of it. Cotton fabric is a rough, porous substrate produced by interlacing threads (composed of micrometer-sized cellulose fibers) placed perpendicular to each other. Consequently, microscale roughness is naturally provided and further nanoscale roughness is necessary for the formation of hierarchical structure to become superhydrophobic. As demonstrated in the SEM images, graphene coating of cotton was not able to provide nanoscale roughness and only could lower its surface free energy. Therefore, the MTCS was used in order to enhance the surface hydrophobicity of the graphene-coated cotton. The silane treatment could create the secondary nanoscale roughness (i.e. entangled nanofilaments, see Fig. 4c) by the combination of hydrolysis and condensing reactions both in solution as well as on the substrate surface (Shirgholami et al. 2013). Figure 5c shows the photograph of red colored water droplets placed on the PMS-graphene-cotton sample and the corresponding static water CA. The droplets formed a circular shape on the fabric surface. The static CA for the sample was 163° ± 3.4°, which demonstrated that hydrophobic graphene-cotton turned into the superhydrophobic fabric. In addition to increasing hydrophobicity, the PMS nanofilaments had a substantial effect on the stickiness of water droplets. The adhesion force between the fabric and droplets reduced significantly so that the water SHA of 7° showed its self-cleaning properties.

In general, there are two classical situations in wetting a rough surface: the homogeneous interface without any air pockets (Wenzel's state) and the composite interface with air pockets trapped between

the rough details (Cassie's state). Experimentally, the wettability state can be distinguished by whether or not there is light between the liquid and substrate in a microscopic side view. Since cotton fabrics are a porous substrate, they are considered physically heterogeneous (air pockets at the interface), irrespective of their different roughness scales (Balu et al. 2008). Thus, the observed superhydrophobic behavior was expected to be modeled by Cassie's equation (Cassie and Baxter 1944), which assumed that a liquid did not completely wet the rough hydrophobic surface due to the presence of air pockets (composite surface) at the liquid solid interface. In the Cassie's state:

$$\cos\theta_r = f_1\cos\theta - f_2 \quad (1)$$

where θ_r is the observed water CA on a rough, porous surface, θ is the intrinsic water CA on the corresponding smooth surface ($\theta = 104^\circ$ for the smooth PMS surface), f_1 is the liquid/solid contact area divided by the projected area, and f_2 is the liquid/vapor contact area divided by the projected area ($f_1 + f_2 = 1$). According to this equation, the f_2 values of the graphene-cotton and PMS-graphene-cotton samples were 0.76 and 0.94, respectively. These data indicated that the achievement of superhydrophobicity was the main result of the air trapped in the very rough surface of the PMS nanofilaments formed on the PMS-graphene-cotton fibers. Compared to the micro-scale graphene-cotton fabric, the very low SHA of the PMS-graphene-cotton was attributed to the complete surface coverage of the graphene-cotton fibers with the very rough PMS nanofilaments, which increased in the amount of air trapped between them and reduced the level of contact with droplets and fibers (Shirgholami et al. 2013). Consequently, the suspended water drops were placed on top of the rough nanofilaments with air pockets beneath them and could rotate smoothly and continuously on the tilted surface.

Deposition of the graphene on the fiber surfaces converted the cotton fabric into an electroconductive substrate, presumably due to the conductive paths formed by the graphene sheets interconnected with each other. The average value of electrical resistivity for the graphene-cotton fabric was calculated as 91.8 k Ω /sq. The graphene-coated fabric was very flexible and graphene layer could not brittle and cracks easily under bending stress and the conductivity value did not change after repeated bending. After coating fabric with the PMS nanofilaments (PMS-graphene-cotton), the

Table 2 Surface resistance varies with different cycles of the coating

Cycles of the coating	Surface resistance (k Ω /sq)
1	400.2
5	12.6
10	3.4
15	1.3
20	0.84

electrical resistivity increased by about 20 % and reached 112.5 k Ω /sq (conductivity decreased). This increase was possibly due to the formation of insulating polysiloxane material on the graphene layer (Wang et al. 2011). However, the increased electrical resistivity was very low, which was not an obstacle for its further applications.

Increasing the number of coating process could result in significant improvement in loading of GO nanosheets and thus increase in the electrical conductivity of the graphene-coated fabric. Table 2 presents the electrical resistivity of the graphene-coated fabric as a function of coating cycles. The electrical resistivity decreased with the increasing number of coating processes and, consequently, electrical properties of the graphene-coated fabric could be easily controlled.

The prepared electroconductive fabrics were expected to have high potential for being used in many technical applications such as electrostatic discharge, electromagnetic interference shielding, heating, wearable electronics, super-capacitors, sensors and actuators, electroluminescent devices and other technologies, requiring both extreme liquid repellency and high electrical conductivity.

Conclusion

This work provided a simple methodology for the fabrication of superhydrophobic cotton cellulose with the ability of electrical conductivity using graphene nanosheets. It was demonstrated that a dip-pad-dry coating of GO dispersion followed by chemical reduction and combined with a subsequent reaction with the MTCS can convert highly water-absorbing insulator cotton fabrics into textile-based substrate conductors with superhydrophobicity properties. The

wettability of cotton fabric changed from superhydrophilicity to hydrophobicity, CA of $143.2^\circ \pm 2.9^\circ$, and then to superhydrophobicity, CA of $163^\circ \pm 3.4^\circ$, due to the coating of fibers with the graphene and the PMS nanofilaments, respectively. The superhydrophobicity of the obtained hybrid fabric was derived from the lotus-like structure with hierarchical roughness, where microscale roughness was produced owing to cellulose fibers while nanoscopic roughness was created by the PMS nanofilaments with the size of 30–90 nm. The graphene-coated fabric showed conductivity with the electrical resistivity of 91.8 k Ω /sq, which increased about 20 % and reached to 112.5 k Ω /sq, after coating with the PMS nanofilaments. Due to the unique structure, the obtained fabrics are very promising to create advanced cellulosic textiles with new and useful functions and properties. Moreover, considering the easy assembling and scalability, it is believed that this method can shed new light on the fabrication of novel graphene-based multifunctional textiles.

References

- AATCC Technical Manual (2007) Test method 76-2005: Electrical surface resistivity of fabrics. American association of textile chemists and colorists, USA
- Allen MJ, Tung VC, Kaner RB (2009) Honeycomb carbon: a review of graphene. *Chem Rev* 110(1):132–145. doi: [10.1021/cr900070d](https://doi.org/10.1021/cr900070d)
- Athauda T, Ozer R (2012) Investigation of the effect of dual-size coatings on the hydrophobicity of cotton surface. *Cellulose* 19(3):1031–1040. doi: [10.1007/s10570-012-9659-7](https://doi.org/10.1007/s10570-012-9659-7)
- Balu B, Breedveld V, Hess DW (2008) Fabrication of “Roll-off” and “Sticky” Superhydrophobic cellulose surfaces via plasma processing. *Langmuir* 24(9):4785–4790. doi: [10.1021/la703766c](https://doi.org/10.1021/la703766c)
- Cassie ABD, Baxter S (1944) Wettability of porous surfaces. *Trans Faraday Soc* 40:546–551. doi: [10.1039/TF9444000546](https://doi.org/10.1039/TF9444000546)
- Cervin N, Aulin C, Larsson P, Wågberg L (2012) Ultra porous nanocellulose aerogels as separation medium for mixtures of oil/water liquids. *Cellulose* 19(2):401–410. doi: [10.1007/s10570-011-9629-5](https://doi.org/10.1007/s10570-011-9629-5)
- Chen H, Müller MB, Gilmore KJ, Wallace GG, Li D (2008) Mechanically strong, electrically conductive, and bio-compatible graphene paper. *Adv Mater* 20(18):3557–3561. doi: [10.1002/adma.200800757](https://doi.org/10.1002/adma.200800757)
- Ganesh VA, Raut HK, Nair AS, Ramakrishna S (2011) A review on self-cleaning coatings. *J Mater Chem* 21(41):16304–16322. doi: [10.1039/C1JM12523K](https://doi.org/10.1039/C1JM12523K)
- Hu L, Cui Y (2012) Energy and environmental nanotechnology in conductive paper and textiles. *Energy Environ Sci* 5(4):6423–6435. doi: [10.1039/C2EE02414D](https://doi.org/10.1039/C2EE02414D)

- Hu L, Pasta M, Mantia FL, Cui L, Jeong S, Deshazer HD, Choi JW, Han SM, Cui Y (2010) Stretchable, porous, and conductive energy textiles. *Nano Lett* 10(2):708–714. doi: [10.1021/nl903949m](https://doi.org/10.1021/nl903949m)
- Hu B, Li D, Manandharm P, Fan Q, Kasilingam D, Calvert P (2012a) CNT/conducting polymer composite conductors impart high flexibility to textile electroluminescent devices. *J Mater Chem* 22(4):1598–1605. doi: [10.1039/C1JM14121J](https://doi.org/10.1039/C1JM14121J)
- Hu P, Wang H, Zhang Q, Li Y (2012b) An indium tin oxide conductive network for flexible electronics produced using a cotton template. *J Phys Chem C* 116(19):10708–10713. doi: [10.1021/jp3005647](https://doi.org/10.1021/jp3005647)
- Huang X, Yin Z, Wu S, Qi X, He Q, Zhang Q, Yan Q, Boey F, Zhang H (2011) Graphene-based materials: synthesis, characterization, properties, and applications. *Small* 7(14):1876–1902. doi: [10.1002/sml.201002009](https://doi.org/10.1002/sml.201002009)
- Huang T, Lu R, Su C, Wang H, Guo Z, Liu P, Huang Z, Chen H, Li T (2012) Chemically modified graphene/polyimide composite films based on utilization of covalent bonding and oriented distribution. *ACS Appl Mater Interfaces* 4(5):2699–2708. doi: [10.1021/am3003439](https://doi.org/10.1021/am3003439)
- Hummers WS, Offeman RE (1958) Preparation of graphitic oxide. *J Am Chem Soc* 80(6):1339. doi: [10.1021/ja01539a017](https://doi.org/10.1021/ja01539a017)
- Li W, Tang X-Z, Zhang H-B, Jiang Z-G, Yu Z-Z, Du X-S, Mai Y-W (2011) Simultaneous surface functionalization and reduction of graphene oxide with octadecylamine for electrically conductive polystyrene composites. *Carbon* 49(14):4724–4730. doi: [10.1016/j.carbon.2011.06.077](https://doi.org/10.1016/j.carbon.2011.06.077)
- Lin Y, Ehlert GJ, Bukowsky C, Sodano HA (2011) Superhydrophobic functionalized graphene aerogels. *ACS Appl Mater Interfaces* 3(7):2200–2203. doi: [10.1021/am200527j](https://doi.org/10.1021/am200527j)
- Luong ND, Pahmanolis N, Hippel U, Korhonen JT, Ruokolainen J, Johansson L-S, Nam J-D, Seppala J (2011) Graphene/cellulose nanocomposite paper with high electrical and mechanical performances. *J Mater Chem* 21(36):13991–13998. doi: [10.1039/C1JM12134K](https://doi.org/10.1039/C1JM12134K)
- Park S, Lee K-S, Bozoklu G, Cai W, Nguyen ST, Ruoff RS (2008) Graphene oxide papers modified by divalent ions—enhancing mechanical properties via chemical cross-linking. *ACS Nano* 2(3):572–578. doi: [10.1021/nn700349a](https://doi.org/10.1021/nn700349a)
- Peng M, Guo H, Liao Z, Qi J, Zhou Z, Fang Z, Shen L (2012) Percolation-dominated superhydrophobicity and conductivity for nanocomposite coatings from the mixtures of a commercial aqueous silica sol and functionalized carbon nanotubes. *J Colloid Interface Sci* 367(1):225–233. doi: [10.1016/j.jcis.2011.10.029](https://doi.org/10.1016/j.jcis.2011.10.029)
- Pereira C, Alves C, Monteiro A, Magén C, Pereira AM, Ibarra A, Ibarra MR, Tavares PB, Araújo JP, Blanco G, Pintado JM, Carvalho AP, Pires J, Pereira MFR, Freire C (2011) Designing novel hybrid materials by one-pot co-condensation: from hydrophobic mesoporous silica nanoparticles to superamphiphobic cotton textiles. *ACS Appl Mater Interfaces* 3(7):2289–2299. doi: [10.1021/am200220x](https://doi.org/10.1021/am200220x)
- Saini P, Choudhary V, Vijayan N, Kotnala RK (2012) Improved electromagnetic interference shielding response of poly(aniline)-coated fabrics containing dielectric and magnetic nanoparticles. *J Phys Chem C* 116(24):13403–13412. doi: [10.1021/jp302131w](https://doi.org/10.1021/jp302131w)
- Schindler WD, Hauser PJ (2004) Chemical finishing of textiles. Woodhead Publishing, Oxford
- Shateri Khalil-Abad M, Yazdanshenas ME (2010) Superhydrophobic antibacterial cotton textiles. *J Colloid Interface Sci* 351(1):293–298. doi: [10.1016/j.jcis.2010.07.049](https://doi.org/10.1016/j.jcis.2010.07.049)
- Shirgholami MA, Shateri Khalil-Abad M, Khajavi R, Yazdanshenas ME (2011) Fabrication of superhydrophobic polymethylsilsesquioxane nanostructures on cotton textiles by a solution-immersion process. *J Colloid Interface Sci* 359(2):530–535. doi: [10.1016/j.jcis.2011.04.031](https://doi.org/10.1016/j.jcis.2011.04.031)
- Shirgholami MA, Shateri-Khalilabad M, Yazdanshenas ME (2013) Effect of reaction duration in the formation of superhydrophobic polymethylsilsesquioxane nanostructures on cotton fabric. *Text Res J* 83(1):100–110. doi: [10.1177/0040517512444335](https://doi.org/10.1177/0040517512444335)
- Simončič B, Tomšič B, Černe L, Orel B, Jerman I, Kovač J, Žerjav M, Simončič A (2012) Multifunctional water and oil repellent and antimicrobial properties of finished cotton: influence of sol-gel finishing procedure. *J Sol Gel Sci Technol* 61(2):340–354. doi: [10.1007/s10971-011-2633-2](https://doi.org/10.1007/s10971-011-2633-2)
- Tang H, Ehlert GJ, Lin Y, Sodano HA (2011) Highly efficient synthesis of graphene nanocomposites. *Nano Lett* 12(1):84–90. doi: [10.1021/nl203023k](https://doi.org/10.1021/nl203023k)
- Tang Z, Kang H, Shen Z, Guo B, Zhang L, Jia D (2012) Grafting of polyester onto graphene for electrically and thermally conductive composites. *Macromolecules* 45(8):3444–3451. doi: [10.1021/ma300450t](https://doi.org/10.1021/ma300450t)
- Wang S, Zhang Y, Abidi N, Cabrales L (2009) Wettability and surface free energy of graphene films. *Langmuir* 25(18):11078–11081. doi: [10.1021/la901402f](https://doi.org/10.1021/la901402f)
- Wang H, Xue Y, Lin T (2011) One-step vapour-phase formation of patternable, electrically conductive, superamphiphobic coatings on fibrous materials. *Soft Matter* 7(18):8158–8161. doi: [10.1039/TF9444000546](https://doi.org/10.1039/TF9444000546)
- Wang J-N, Shao R-Q, Zhang Y-L, Guo L, Jiang H-B, Lu D-X, Sun H-B (2012) Biomimetic graphene surfaces with superhydrophobicity and iridescence. *Chem Asian J* 7(2):301–304. doi: [10.1002/asia.201100882](https://doi.org/10.1002/asia.201100882)
- Yan YY, Gao N, Barthlott W (2011) Mimicking natural superhydrophobic surfaces and grasping the wetting process: a review on recent progress in preparing superhydrophobic surfaces. *Adv Colloid Interface* 169(2):80–105. doi: [10.1016/j.cis.2011.08.005](https://doi.org/10.1016/j.cis.2011.08.005)
- Yu G, Hu L, Vosgueritchian M, Wang H, Xie X, McDonough JR, Cui X, Cui Y, Bao Z (2011) Solution-processed graphene/MnO₂ nanostructured textiles for high-performance electrochemical capacitors. *Nano Lett* 11(7):2905–2911. doi: [10.1021/nl2013828](https://doi.org/10.1021/nl2013828)
- Zimmermann J, Seeger S, Reifler FA (2009) Water shedding angle: a new technique to evaluate the water-repellent properties of superhydrophobic surfaces. *Text Res J* 79(17):1565–1570. doi: [10.1177/0040517509105074](https://doi.org/10.1177/0040517509105074)
- Zou D, Lv Z, Cai X, Hou S (2012) Macro/microfiber-shaped electronic devices. *Nano Energy* 1(2):273–281. doi: [10.1016/j.nanoen.2012.01.005](https://doi.org/10.1016/j.nanoen.2012.01.005)